Observing periodic gap variations in cuprates

Riju Banerjee, ^{1,3,*,†} Emily L. Wang ^{1,2,3,*} and Eric W. Hudson ^{3,‡}

**Inational Physical Laboratory, Teddington TW11 0LW, United Kingdom

**Department of Computer Science, Northwestern University, Evanston, Illinois 60201, USA

**Department of Physics, The Pennsylvania State University, University Park, Pennsylvania 16802, USA

(Received 29 January 2024; revised 2 July 2024; accepted 26 September 2024; published 2 December 2024)

The presence of multiple orders in strongly correlated electronic materials like the cuprate superconductors, coupled with spatial inhomogeneity, poses a challenge to the interpretation of spectroscopic data taken on them. Here, we present a technique that directly acknowledges these orders and inhomogeneities and extracts statistically significant features from such data. Applying this technique to scanning tunneling spectroscopy measurements from single and bilayer cuprates spanning a wide doping range, we peer through local inhomogeneities and identify a gaplike feature that breaks translational and rotational symmetries and varies periodically in a fourfold pattern. This identification of spectral features aligns well with theoretical predictions of spatially modulated pair density.

DOI: 10.1103/PhysRevB.110.224501

I. INTRODUCTION

Materials with strong electronic correlations often feature a plethora of electronic orders that coexist or compete with each other. Strong electron-electron interactions, acting through spin, charge, or orbital or lattice degrees of freedom, result in a highly inhomogeneous electronic structure experimentally found to be ubiquitous in these materials [1]. For example, one of the most heavily studied strongly correlated systems, the high temperature superconductor cuprates, has been shown to exhibit signatures of electronic phase separation [2], nematicity [3,4], checkerboard patterns [5,6], and other local order [7], while also exhibiting local inhomogeneities, perhaps seeded by disorder [8], in transition temperature T_c [9], particle-hole asymmetry [10], and Fermi surface [11]. Unfortunately, to date, it has been impossible to find a consistent theoretical description encompassing all the intertwined orders in these materials. Indeed, theoretically modeling this omnipresent inhomogeneous electronic order is so challenging that it is usually simply ignored.

Some of the most significant evidence of inhomogeneity in cuprates has been gathered through scanning tunneling microscopy (STM). The single particle tunneling spectrum [Fig. 1(a)] is often reminiscent of what would be expected for a d-wave superconductor, with a v-shaped gap, symmetric about the Fermi energy, and peaked at the maximum gap

Published by the American Physical Society under the terms of the Creative Commons Attribution 4.0 International license. Further distribution of this work must maintain attribution to the author(s) and the published article's title, journal citation, and DOI.

energy Δ . Extracting this peak energy, either algorithmically [2] or via some fitting technique [12,13], is a common first analysis step, and a spatial map of the energy of this feature [a "gap map," as shown in Fig. 1(b)] further highlights the inhomogeneity in these materials. However, other spectral features besides this peak also exist, including higher energy features, which are usually extremely challenging to measure, but were found to be tied closely to nonstoichiometric oxygen atom dopants [8], and a lower energy "kink" [Fig. 1(a)], often hidden by the more dominant peak feature. More than a decade ago, one of us (E.W.H.) argued [14] the peak energy to be associated with the pseudogap (a nonsuperconducting order in the material) and the kink with superconductivity, and these two spectroscopic features are often labeled accordingly as Δ_{PG} and Δ_{SC} , even though such an interpretation is still somewhat debated [15,16].

Interestingly, within this strongly spatially inhomogeneous single-particle spectrum, both uniformity and order have also been observed. The same spectral surveys [measurements of the energy E and position \vec{r} , dependent differential tunneling conductance $g(E,\vec{r})$] which yield highly inhomogeneous gap maps also reveal, through quasiparticle interference (QPI) studies [17], that the Bogoliubov quasiparticles responsible for superconductivity are well defined and coherent throughout the sample [18]. In contrast to the apparently global orders revealed by QPI, at the level of individual spectra, this coherence of the Bogoliubov quasiparticles (and hence the superconducting order) is also suggested by the uniformity of the kink energy [14], which remains constant defying all underlying electronic inhomogeneity.

These hints of homogeneity are rare, but they confirm the existence of persistent patterns in the cuprate electronic structure, obscured behind the façade of inhomogeneity. Given that, it is perhaps surprising that after several decades of study and multiple theoretical predictions, cuprate gap maps have not revealed any order themselves. For example, pair

^{*}These two authors contributed equally to this work.

[†]Contact author: riju.banerjee@npl.co.uk

[‡]Contact author: ehudson@psu.edu

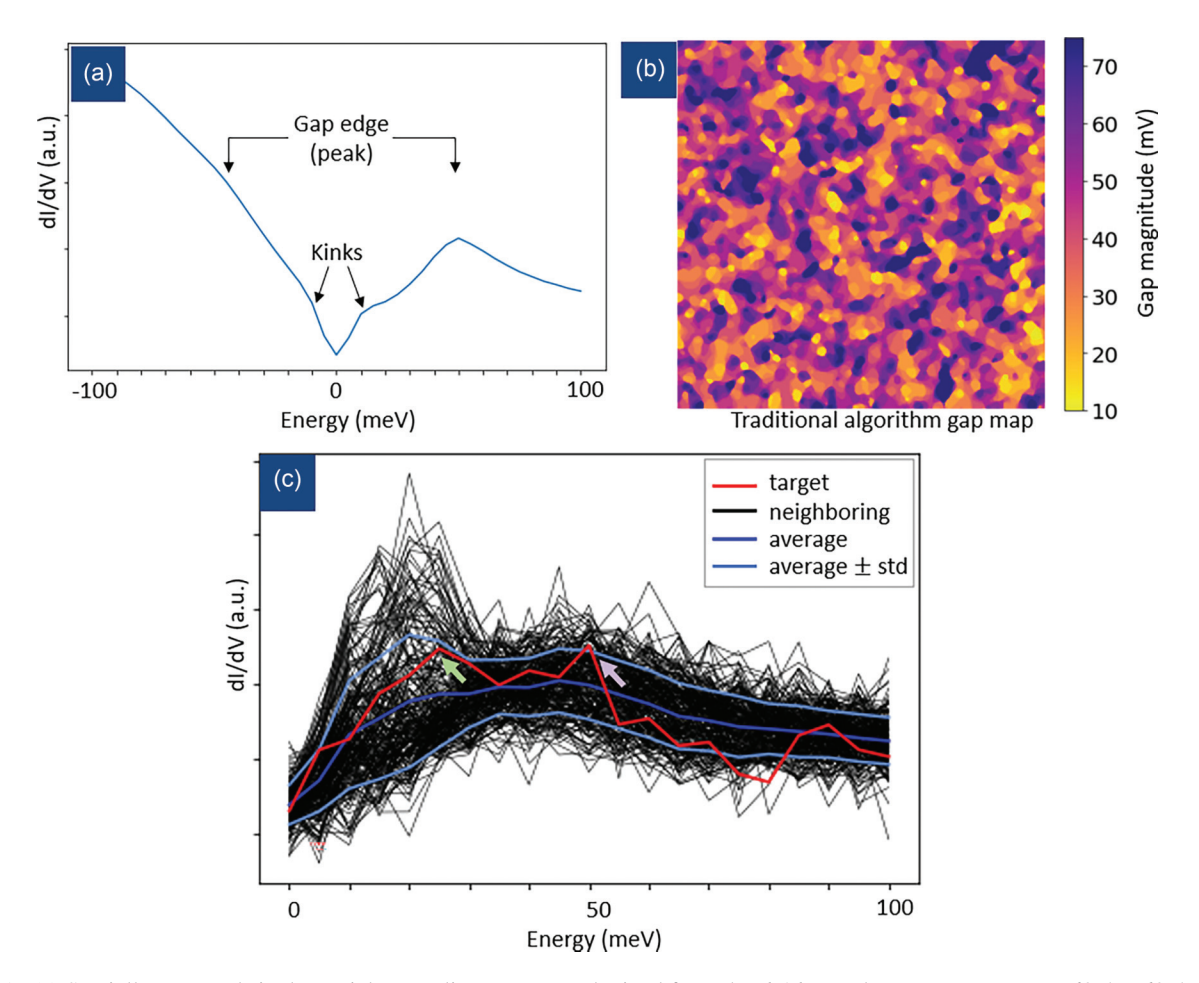


FIG. 1. (a) Spatially averaged single particle tunneling spectrum obtained from the dI/dV conductance maps over a $68.5 \times 68.5 \,\mathrm{mm^2}$ area broken into 400×400 pixels on a region of underdoped Bi-2201 ($T_c = 32 \,\mathrm{K}$). Typical spectral features like the gap, kinks, and the gap edge (peaks) are marked. (b) For the same data set from which (a) was obtained, the traditional "gap" (peak) map algorithm considers each spectrum individually and shows strong local electronic variation without any clear order. (c) The idea behind Statistically Unique Feature Finder (STUFF) algorithm. Each target spectrum (red curve) is compared to approximately two hundred spectra around it (black curves) to identify a z score [Eq. (1)]. For the target spectrum in red, the peak at 25 meV (marked by green arrow) can naively be identified as the gap edge. However, that feature is common to many other neighborhood spectra, suggesting that it might be arising from a local (unidentified) electronic order. Instead, STUFF identifies the peak at 50 meV (marked by violet arrow) as the gap edge as that is a peak feature statistically most unique to the target spectrum. When the algorithm is executed for each spectrum in the field of view, the new gap map obtained from STUFF is shown in Fig. 2(b). Spectral survey parameters were $I_s = 400 \,\mathrm{pA}$ and $V_{\mathrm{bias}} = -200 \,\mathrm{mV}$.

density wave (PDW) models, built on a decades old theoretical paradigm that has recently gathered considerable experimental support, specifically predict spatial, periodic gap variation [19–25]. Here, we introduce a technique to disentangle the gap (spectral peak) energy from underlying inhomogeneities, and find that the spectral peak does indeed vary in a fourfold symmetric pattern and that its interplay with the kink is responsible for the appearance of the checkerboard pattern [26,27] at low energies.

II. STATISTICALLY UNIQUE FEATURE FINDER

Conventional gap-finding algorithms analyze each spectrum individually, either algorithmically searching for sudden changes in density of states (peaks) or slopes to identify the gap edge, or by using a curve fitting technique [2,12,13]. However, such a strategy can be negatively impacted by inhomogeneity, particularly if local dopants or defects and various

orders contribute to the electronic structure. To get around this issue, we have developed the Statistically Unique Feature Finder (STUFF), which compares each spectrum to others nearby (within a few nanometers), in order to find spectral features as they appear given the local background.

The idea behind STUFF is demonstrated in Fig. 1(c), where it is applied on an underdoped Bi-2201 ($T_c = 32 \text{ K}$) sample. The sample also has Pb dopants to reduce structural supermodulations [28,29]. Considering the (arbitrarily chosen) target spectrum shown in red, we see that there is a peak near 25 meV (only the positive bias half is shown), which is identified by the traditional algorithm as the gap edge. However, considering more than two hundred spectra obtained in a $2.4 \times 2.4 \,\mathrm{nm^2}$ neighborhood (shown in black), we find they all have a comparable peaklike feature around the same energy. This suggests that this particular feature might be arising from an unidentified background order. Examining the target spectrum, we see that there is another distinct

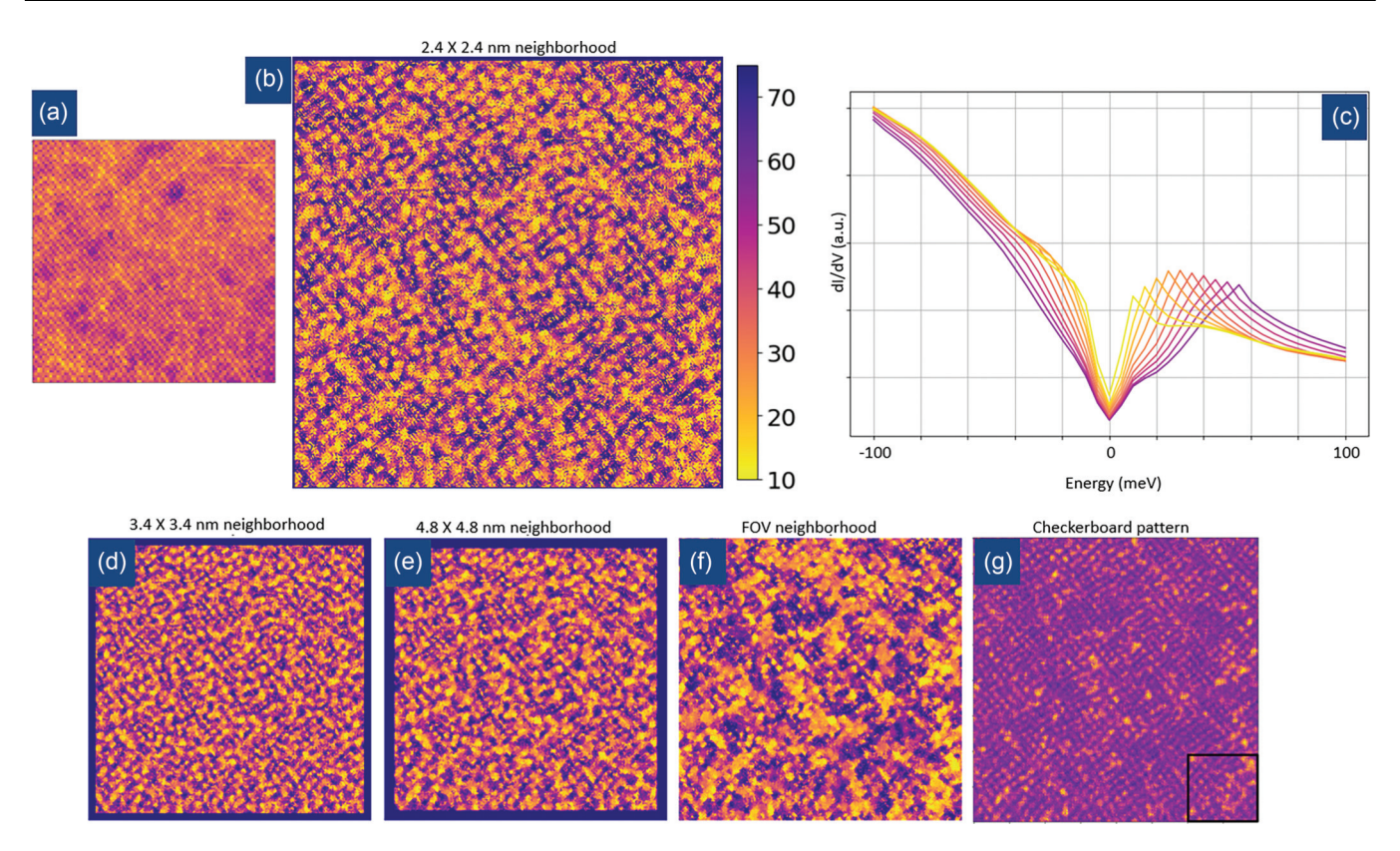


FIG. 2. (a) Atomic resolution topography shows the lack of any supermodulation in the Pb doped Bi-2201 ($T_c = 32 \text{ K}$) sample. (b) Redrawn gap map obtained from our STUFF algorithm using a 2.4×2.4 nm (14 pixels square) neighborhood. Note the emergence of a clear fourfold symmetric pattern, in contrast to the lack of any order detected by the traditional algorithm [Fig. 1(b)], with the spatially average spectra corresponding to the colors plotted in (c). The color bar is shared across images (b)–(g) and is the same as in Fig. 1(b). (d)–(f) Increasing the neighborhood size considered for calculating the z score does not change the periodicity of the fourfold symmetric pattern, but the pattern gets blurred and gradually morphs towards the traditional gap map [Fig. 1(b)]. (g) 10-meV layer of the spectral map, demonstrating fourfold symmetry of the checkerboard pattern. The black box marks the region of the atomic resolution topography in (a). The field of view in (b), (d)–(f), and (g) is the same as in Fig. 1(b), i.e., $68.5 \times 68.5 \times m^2$.

peaklike feature around 50 meV, which is absent in other spectra taken from the same region. STUFF thus identifies this peak energy, as it is a statistically unique peak feature specific to the target spectrum.

In practice, STUFF is implemented by calculating a z score for each spectrum g(E) as

$$z(E) = \frac{g(E) - \bar{g}(E)}{\sigma(E)},\tag{1}$$

where $\bar{g}(E)$ is the average spectrum of the neighborhood [shown in dark blue in Fig. 1(c)] and $\sigma(E) = \sqrt{\frac{1}{N}\sum_{i=1}^{N}{[g_i(E) - \bar{g}(E)]^2}}$ is the standard deviation of all N spectra in its neighborhood, describing the local variation at each energy. We note that for the target spectrum [red in Fig. 1(c)], the z score will be highest for the feature at 50 meV (marked by a violet arrow), consistent with the observation above. Thus, the STUFF algorithm selects out peaklike features unique to the target spectrum by comparing it to its neighboring spectra. We run the STUFF algorithm for every spectrum in the field of view (FOV) and determine the energy for which the z score is the highest for each spectrum. To preserve consistency with previous work, we will refer to this identified peak energy (for each spectrum, the energy for which the z score is highest) as "the gap" Δ_{ST} , and note that it

is very similar to "the pseudogap energy" Δ_{PG} determined by conventional techniques. Finally, we use this identified peak energy for each spectrum to redraw the gap map.

III. RESULTS FROM STUFF

We apply this technique to two different cuprates, underdoped Bi-2201 ($T_c = 32 \text{ K}$) and overdoped Bi-2212 ($T_c = 75$ K). Both samples are doped with Pb to reduce the structural supermodulation that exists in the undoped materials and can also result in periodic gap variations [30,31] [Fig. 2(a)]. The samples were studied at 4 K using a custom-built variabletemperature scanning tunneling microscope. The spectral surveys were corrected for thermal drift [32]. Our analysis reveals that for both samples the gap varies spatially in a fourfold symmetric pattern [Fig. 2(b)], which was not evident using the conventional gap-finding algorithm [Fig. 1(b)]. Average spectra for each gap value are shown in Fig. 2(c) using the same color indexing scheme used in Fig. 2(b). The fanning out of these spectra, with gaps from 10 to 65 meV, is essentially indistinguishable from similar analysis using the conventional algorithm [5,14], making the dramatic difference in the spatial gap map even more remarkable.

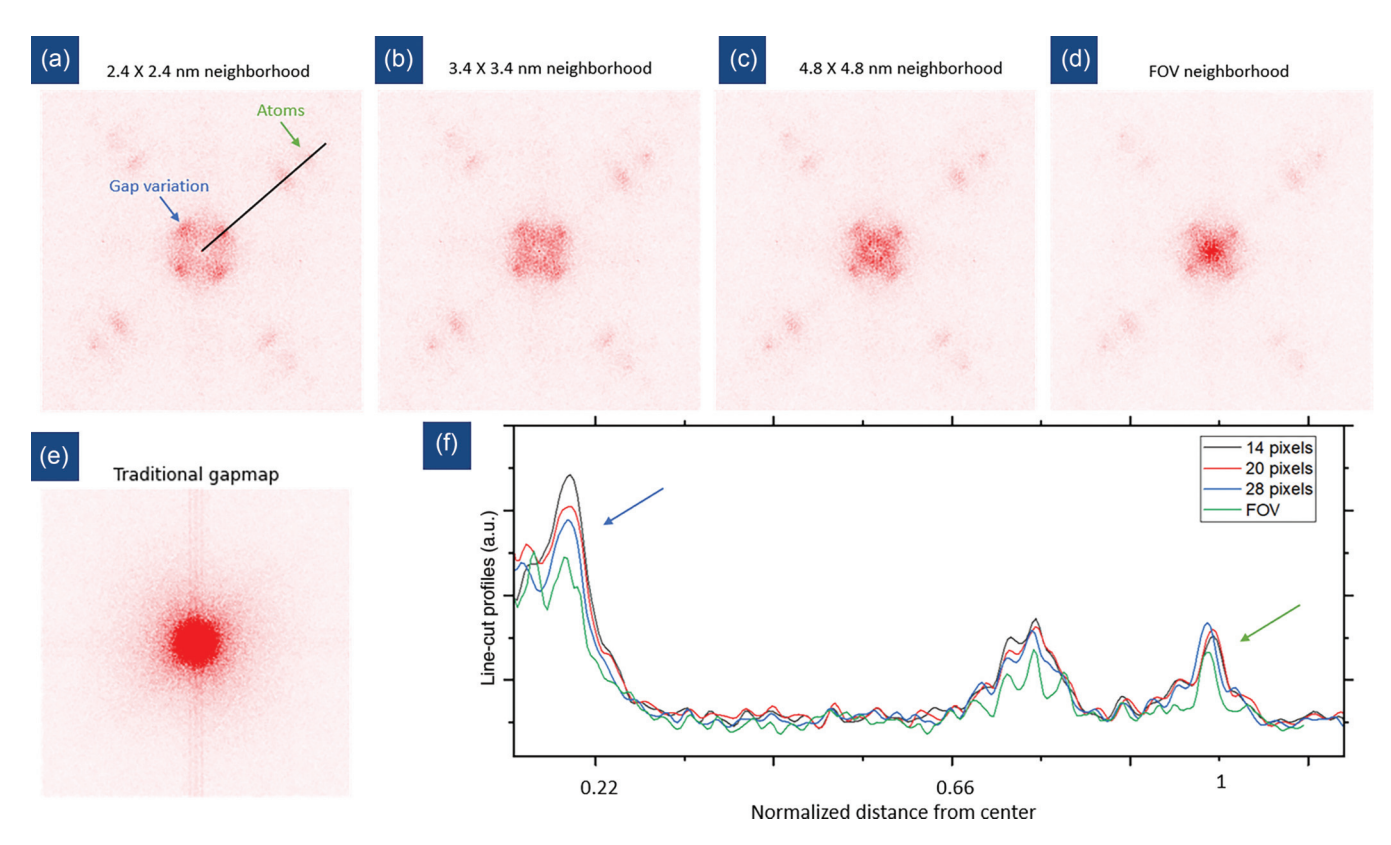


FIG. 3. FFTs of the gap maps obtained from STUFF and shown in Fig. 2. (a)—(d) A clear fourfold symmetric gap variation pattern emerges using our STUFF algorithm, whose periodicity is marked by blue arrow. In contrast, the FFT of the traditional gap map, shown in (e), has no periodicity. STUFF is also able to pick out the atomic periodicity (green arrow). Note that observed periodicity of the fourfold symmetric gap variation pattern does not depend on the size of the neighborhood considered for running the STUFF algorithm, implying that the periodicity is inherent to the sample, and not an artifact of the algorithm. However, increasing the neighborhood size does reduce STUFF's efficacy, as seen in the progressive transfer of weight from the peaks to the center, leading to a reduction in peak height shown in (f).

From Eq. (1), it follows that the only free parameter in our technique is the size of the neighborhood we consider in calculating the z score (varying the number of neighborhood spectra, N). We next check that our observation of periodic gap variation is not an artifact of partitioning the spectral map into these smaller regions. The effect of changing the neighborhood size is demonstrated in Figs. 2(d)-2(f). Considering larger and larger neighborhoods, we see that the length scale of gap variation is insensitive to the size of the neighborhood. Remarkably however, as the neighborhood size is increased, and each spectrum is compared to a larger number of spectra around it, identifying the gaplike feature becomes harder and harder, causing the fourfold symmetric pattern to gradually become weaker. When the neighborhood is increased to the entire field of view, the gap map from STUFF approaches the traditional gap map algorithm shown in Fig. 1(b). In Supplemental Material Sec. 1 [33], we present a similar analysis on another sample, Bi-2212 ($T_c = 75$ K) and make similar observations. We also note that the fourfold symmetric pattern looks similar to the well-known checkerboard pattern [Fig. 2(g)], hinting at a possible relation between the two, which we address later in the paper.

The fact that the length scale of gap variation is not an artifact of our analysis is further demonstrated in Figs. 3(a)–3(d) where we show fast Fourier transforms (FFTs) of the gap maps in Figs. 2(d)–2(g). Line cuts taken through the

symmetric axis [marked by the black line in Figs. 3(a)–3(d)] demonstrate that increasing the neighborhood only reduces the contrast of the fourfold symmetric pattern, without changing its periodicity. We also note the progressive increase in weight in the center of the FFT pattern in Figs. 3(a)–3(d). The center of the FFT corresponds to aperiodic features (noise), and that increases as STUFF's efficiency is reduced.

We next note that even though STUFF reveals a clear fourfold symmetric gap variation, the size of the gap still varies considerably throughout the sample, similar to the traditional gap-map algorithm. This is manifested as local variations in contrast in Fig. 2(b). We now turn to understanding how the gap changes as a function of the local strength of the fourfold symmetric wave. Identifying the peaks in the fourfold symmetric pattern [Fig. 2(b)], we break the field of view into Voronoi cells and color (bin) them in five different groups depending on the gap size near the center of each cell [Fig. 4(a)]. The groups are colored blue, orange, green, red, and violet respectively in order of increasing gap size at the cell center. Further subdividing each Voronoi cell into six concentric spatial regions, we show intracell gap variations in Fig. 4(b). Cells with smaller gaps near the center (in blue) show greater intracell gap variation than cells with larger gaps in their center (violet). In Figs. 4(c) and 4(d), we plot the average spectra for the different distance groups showing this intracell gap variation. Plots with light to dark show the variation from the

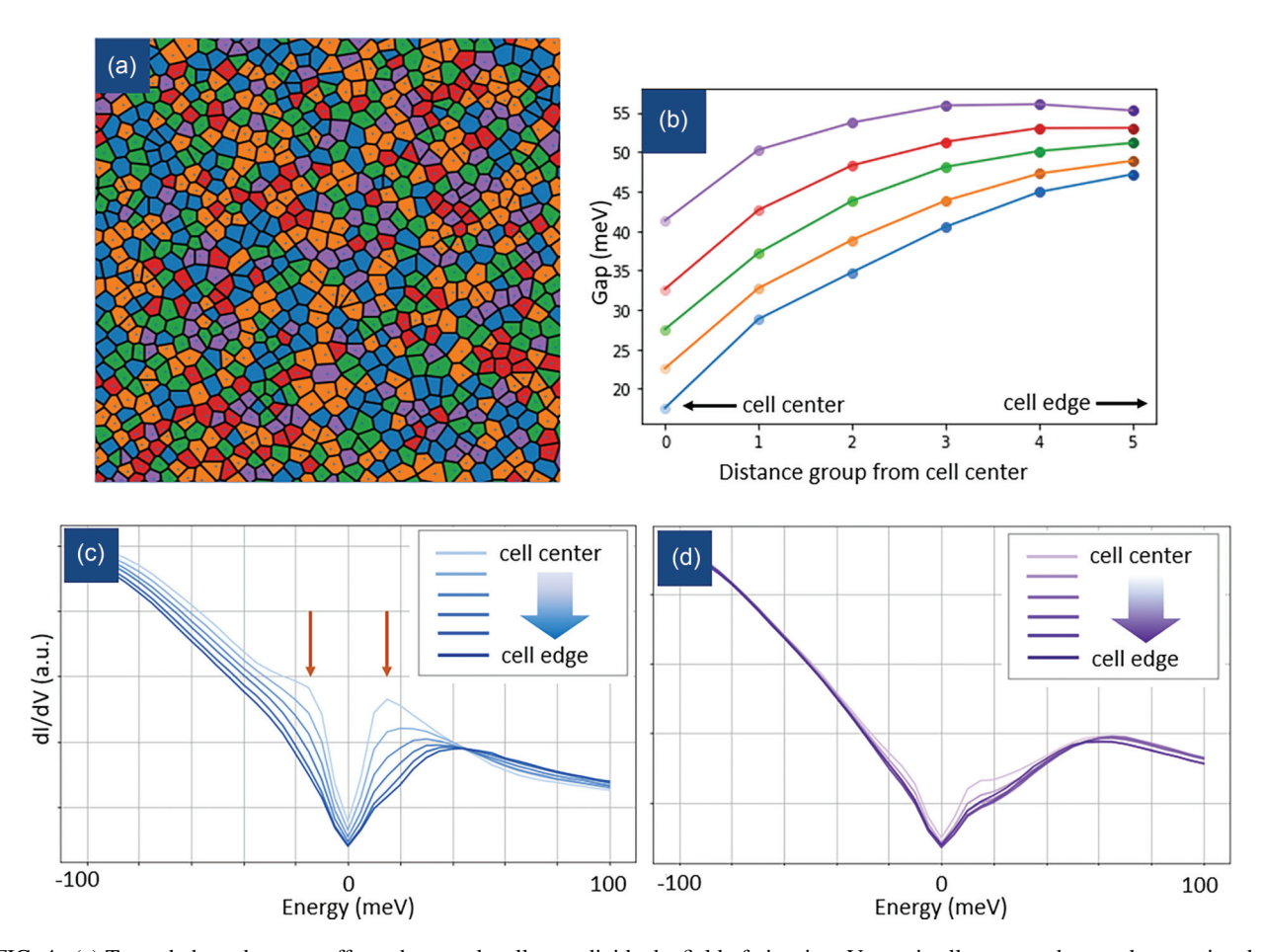


FIG. 4. (a) To study how the wave affects the gaps locally, we divide the field of view into Voronoi cells, centered on peaks associated with the fourfold symmetric pattern, and bin them into five different groups depending on the gap magnitude at the cell center. As shown in Fig. 2, the cells have smaller gaps near the center and larger gaps towards their edges. The colors blue, orange, green, red, and violet indicate the gap size at the cell center in increasing order. (b) More gap variation is seen in cells with smaller gaps near the center. This implies a "sea" of large gaps being broken into fourfold symmetric "islands" of smaller gapped regions. Panels (c) and (d) show the average spectra of the Voronoi cells with smallest (colored blue) and largest (colored violet) gaps near the centers. Note that in (c), for islands with small gaps, significantly prominent peaks are seen (marked by brown arrows) compared to islands with large gaps in (d).

cell center to its boundary. Note that the spectra farther away from the cell centers [dark blue and dark purple in Figs. 4(c) and 4(d) respectively] are similar. This implies that the electronic distribution in the sample has a large gap "sea" which is broken up into "island" regions with smaller gaps arranged in a fourfold symmetric pattern. This picture is similar to an electronic phase separation idea hypothesized decades ago [2]. Further research would be required to understand what creates the small gap islands and how they remain segregated from the large gap sea regions.

IV. INTERPRETATIONS AND RELATION TO PDW AND PSEUDOGAP

Amidst all the caveats concerning various aspects of cuprates, it is generally agreed that there are two electronic phases that occur simultaneously, namely superconductivity and pseudogap. Understanding the origin of these two phases and how they compete, cooperate, or merely coexist with each other has been the subject of intense debate over the past several decades. Recent experimental evidence [19–24] has suggested that the physics of cuprates and other high

temperature superconductors can be explained by pair density waves (PDWs). In fact, several theoretical studies have also hypothesized that the PDW is the "parent order" in these materials, from which other orders like pseudogap and the checkerboard order naturally emerge [34–36]. As our observation of a periodic gap variation aligns well with the predictions of bidirectional PDWs, we next turn to examining our observations in light of different proposed pseudogap and PDW theories.

We note that our observation of a fourfold symmetric gap map looks very similar to the checkerboard pattern, which arises from the periodic variation of the spectral weight (density of states) at low energies. One of the earliest attempts to explain the checkerboard pattern was using a spatially varying gap arising from a PDW [19,21,37–39]. We next argue that the periodic gap variation obtained from STUFF results in a corresponding periodic variation of the low energy spectral weight and can thus explain the origin of the checkerboard pattern. In plotting the group average spectra obtained from our STUFF algorithm in Fig. 2(c), we see that all of them have a distinct kink at 10 meV. This observation suggests that there are in fact two distinct gaps, originating from the

superconducting gap (Δ_{SC} , visible as a kink and which remains constant throughout) and the pseudogap (Δ_{PG} , which varies periodically) phases. As the STUFF algorithm selects out only the locally varying parameter, ignoring local uniformities, we identify the STUFF gap $\Delta_{ST} = \Delta_{PG}$. Figure 4 demonstrates how close these two gaps are in energy and how they interact with each other. In regions where $\Delta_{PG} \gg$ Δ_{SC} , the two gaps are clearly distinguishable in the average spectra [Fig. 4(d)]. In contrast, in regions where $\Delta_{PG} \approx \Delta_{SC}$, the interaction between the two energy scales results in high coherence peaks [Fig. 4(c)] and increased spectral weight in the gap in both Bi-2201 and Bi-2212 samples (see Supplemental Material Sec. 1 [33] for Bi-2212 data). It is then straightforward to realize that the periodic gap variation can result in periodic low-bias conductance variation, resulting in a checkerboard pattern. Thus, the checkerboard pattern is but a low energy manifestation of a spatially varying pseudogap, which varies over a much wider energy range. Our observations likely also explain why the checkerboard pattern is much easier to observe directly in STS than the gap variation itself. This is likely because all the variation of Δ_{PG} and inhomogeneities must necessarily stay sufficiently outside of the superconducting gap (leaving it uniform) to have a welldefined gap everywhere and hence a superconductor.

In the above discussion, we argued that the spatially varying gap observed from STUFF is related to the pseudogap Δ_{PG} and showed how it interacts with the spatially uniform superconducting gap, Δ_{SC} , to create the checkerboard pattern. Quantum oscillations (like the checkerboard) in the pseudogap phase is an integral part of cuprate physics [40] and many studies have tried to relate them to the PDW [21,34,35,39,41– 47]. Our observation of a spatially varying pseudogap adds further support to such hypotheses. Another interesting aspect of the pseudogap phase that is generally agreed upon is that the pseudogap strength goes down with increasing doping level, even though the exact pseudogap termination point remains debatable. In Supplemental Material Sec. 2 [33], we present the result of STUFF algorithm on two more Bi-2201 samples with higher hole doping. We show that compared to the underdoped ($T_c = 32 \text{ K}$) sample, the gap variation pattern is significantly weakened for the optimally doped ($T_c = 35 \text{ K}$, Fig. S2) sample and almost imperceptible for the overdoped ($T_c = 15$ K, Fig. S3) sample. This weakening of the pattern suggests that the spectral variation observed is related to the pseudogap phase, and is consistent with theoretical proposals arguing the existence of a quantum critical point separating an ordered pseudogap and a disordered phase [48–50].

Although a PDW for cuprates was originally hypothesized decades ago [21], it has gathered considerable experimental support in recent years [34,39,43–45,51]. To date, several experiments like the onset of c-axis superconductivity in lanthanum based cuprates, like La_{1.85-v}Nd_vSr_{0.15}CuO₄ at temperatures far below T_c [52], spatially periodic variation of Cooper pair density observed by scanning Josephson tunneling microscopy [53], and halving of the charge density wave vector inside vortex halos under magnetic fields [54] have provided considerable, albeit circumstantial evidence for PDW in cuprates and unfortunately only in systems at a single doping level. Due to their strong spatial inhomogeneity, direct observation of gap variation using single particle tunneling in strongly correlated materials is rare [55], and has only been possible indirectly via Josephson tunneling spectroscopy [56]. Our direct observation of spatially periodic gap variation in both single and bilayer cuprates exploring a large doping range adds strong support to the existence of pair density waves in them.

V. METHODS

The samples were cleaved in UHV environment at 77 K and were quickly transferred to a custom-built STM to ensure that the surface remains clean. The samples were studied using a tip cut from a Pt-Ir (80%-20%) wire.

ACKNOWLEDGMENTS

We thank J. C. Davis and J. E. Hoffman groups for Bi-2212 data. We thank A. Tzalenchuk and S. Samaddar for helpful comments. We thank the Department of Physics of The Pennsylvania State University for generous support. In addition, R.B. also thanks the National Physical Laboratory, Teddington, UK for generous support.

^[1] E. Dagotto, Complexity in strongly correlated electronic systems, Science **309**, 257 (2005).

^[2] K. M. Lang, V. Madhavan, J. E. Hoffman, E. W. Hudson, H. Eisaki, S. Uchida, and J. C. Davis, Imaging the granular structure of high- T_c superconductivity in underdoped $\text{Bi}_2\text{Sr}_2\text{CaCu}_2\text{O}_{8+\delta}$, Nature (London) **415**, 412 (2002).

^[3] M. J. Lawler, K. Fujita, J. Lee, A. R. Schmidt, Y. Kohsaka, C. K. Kim, H. Eisaki, S. Uchida, J. C. Davis, J. P. Sethna *et al.*, Intra-unit-cell electronic nematicity of the high-T_c copper-oxide pseudogap states, Nature (London) 466, 347 (2010).

^[4] T.-M. Chuang, M. P. Allan, J. Lee, Y. Xie, N. Ni, S. L. Bud'ko, G. S. Boebinger, P. C. Canfield, and J. C. Davis, Nematic electronic structure in the "parent" state of the iron-based superconductor Ca(Fe_{1-x}Co_x)₂As₂, Science 327, 181 (2010).

^[5] K. McElroy, D.-H. Lee, J. E. Hoffman, K. M. Lang, J. Lee, E. W. Hudson, H. Eisaki, S. Uchida, and J. C. Davis, Coincidence

of checkerboard charge order and antinodal state decoherence in strongly underdoped superconducting $Bi_2Sr_2CaCu_2O_{8+\delta}$, Phys. Rev. Lett. **94**, 197005 (2005).

^[6] T. Hanaguri, C. Lupien, Y. Kohsaka, D.-H. Lee, M. Azuma, M. Takano, H. Takagi, and J. C. Davis, A 'checkerboard' electronic crystal state in lightly hole-doped Ca_{2-x}Na_xCuO₂Cl₂, Nature (London) 430, 1001 (2004).

^[7] M. Vershinin, S. Misra, S. Ono, Y. Abe, Y. Ando, and A. Yazdani, Local ordering in the pseudogap state of the high-*T_c* superconductor Bi₂Sr₂CaCu₂O_{8+δ}, Science 303, 1995 (2004).

^[8] I. Zeljkovic, Z. Xu, J. Wen, G. Gu, R. S. Markiewicz, and J. E. Hoffman, Imaging the impact of single oxygen atoms on superconducting Bi_{2+v}Sr_{2-v}CaCu₂O_{8+x}, Science 337, 320 (2012).

^[9] K. K. Gomes, A. N. Pasupathy, A. Pushp, S. Ono, Y. Ando, and A. Yazdani, Visualizing pair formation on the atomic

- scale in the high-Tc superconductor $Bi_2Sr_2CaCu_2O_{8+\delta}$, Nature (London) **447**, 569 (2007).
- [10] C. Zou, Z. Hao, X. Luo, S. Ye, Q. Gao, M. Xu, X. Li, P. Cai, C. Lin, X. Zhou *et al.*, Particle–hole asymmetric superconducting coherence peaks in overdoped cuprates, Nat. Phys. 18, 551 (2022).
- [11] W. D. Wise, K. Chatterjee, M. C. Boyer, T. Kondo, T. Takeuchi, H. Ikuta, Z. Xu, J. Wen, G. D. Gu, Y. Wang *et al.*, Imaging nanoscale Fermi-surface variations in an inhomogeneous superconductor, Nat. Phys. 5, 213 (2009).
- [12] B. W. Hoogenboom, C. Berthod, M. Peter, Ø. Fischer, and A. A. Kordyuk, Modeling scanning tunneling spectra of Bi₂Sr₂CaCu₂O_{8+δ}, Phys. Rev. B 67, 224502 (2003).
- [13] W. O. Tromp, T. Benschop, J.-F. Ge, I. Battisti, K. M. Bastiaans, D. Chatzopoulos, A. H. M. Vervloet, S. Smit, E. van Heumen, M. S. Golden *et al.*, Puddle formation and persistent gaps across the non-mean-field breakdown of superconductivity in overdoped (Pb, Bi)₂Sr₂CuO_{6+δ}, Nat. Mater. 22, 703 (2023).
- [14] M. C. Boyer, W. D. Wise, K. Chatterjee, M. Yi, T. Kondo, T. Takeuchi, H. Ikuta, and E. W. Hudson, Imaging the two gaps of the high-temperature superconductor Bi₂Sr₂CuO_{6+x}, Nat. Phys. 3, 802 (2007).
- [15] S. Hüfner, M. A. Hossain, A. Damascelli, and G. A. Sawatzky, Two gaps make a high-temperature superconductor? Rep. Prog. Phys. 71, 062501 (2008).
- [16] Y. Noat, A. Mauger, M. Nohara, H. Eisaki, S. Ishida, and W. Sacks, Cuprates phase diagram deduced from magnetic susceptibility: What is the 'true' pseudogap line? Solid State Commun. 348, 114689 (2022).
- [17] J. E. Hoffman, K. McElroy, D.-H. Lee, K. M. Lang, H. Eisaki, S. Uchida, and J. C. Davis, Imaging Quasiparticle Interference in Bi₂Sr₂CaCu₂O_{8+δ}, Science 297, 1148 (2002).
- [18] J. Zaanen, Pebbles in the nodal pond, Nature (London) 422, 569 (2003).
- [19] S. Baruch and D. Orgad, Spectral signatures of modulated d-wave superconducting phases, Phys. Rev. B 77, 174502 (2008).
- [20] A. Himeda, T. Kato, and M. Ogata, Stripe states with spatially oscillating d -wave superconductivity in the two-dimensional t-t'-J model, Phys. Rev. Lett. **88**, 117001 (2002).
- [21] H.-D. Chen, O. Vafek, A. Yazdani, and S.-C. Zhang, Pair density wave in the pseudogap state of high temperature superconductors, Phys. Rev. Lett. 93, 187002 (2004).
- [22] D. F. Agterberg, J. C. S. Davis, S. D. Edkins, E. Fradkin, D. J. Van Harlingen, S. A. Kivelson, P. A. Lee, L. Radzihovsky, J. M. Tranquada, and Y. Wang, The physics of pair-density waves: Cuprate superconductors and beyond, Annu. Rev. Condens. Matter Phys. 11, 231 (2020).
- [23] D. Podolsky, E. Demler, K. Damle, and B. I. Halperin, Translational symmetry breaking in the superconducting state of the cuprates: Analysis of the quasiparticle density of states, Phys. Rev. B 67, 094514 (2003).
- [24] E. Berg, E. Fradkin, and S. A. Kivelson, Charge-4e super-conductivity from pair-density-wave order in certain high-temperature superconductors, Nat. Phys. 5, 830 (2009).
- [25] C. M. Varma, Pseudogap and Fermi arcs in underdoped cuprates, Phys. Rev. B 99, 224516 (2019).
- [26] C. Howald, H. Eisaki, N. Kaneko, M. Greven, and A. Kapitulnik, Periodic density-of-states modulations in superconducting Bi₂Sr₂CaCu₂O_{8+δ}, Phys. Rev. B 67, 014533 (2003).

- [27] W. D. Wise, M. C. Boyer, K. Chatterjee, T. Kondo, T. Takeuchi, H. Ikuta, Y. Wang, and E. W. Hudson, Charge-density-wave origin of cuprate checkerboard visualized by scanning tunnelling microscopy, Nat. Phys. 4, 696 (2008).
- [28] T. Kondo, T. Takeuchi, U. Mizutani, T. Yokoya, S. Tsuda, and S. Shin, Contribution of electronic structure to thermoelectric power in (Bi, Pb)₂(Sr, La)₂CuO_{6+δ}, Phys. Rev. B 72, 024533 (2005).
- [29] I. Chong, T. Terashima, Y. Bando, M. Takano, Y. Matsuda, T. Nagaoka, and K. Kumagai, Growth of heavily Pb-substituted Bi-2201 single crystals by a floating zone method, Phys. C (Amsterdam, Neth.) 290, 57 (1997).
- [30] B. M. Andersen, P. J. Hirschfeld, and J. A. Slezak, Superconducting gap variations induced by structural supermodulation in Bi₂Sr₂CaCu₂O₈, Phys. Rev. B **76**, 020507(R) (2007).
- [31] N. Jenkins, Y. Fasano, C. Berthod, I. Maggio-Aprile, A. Piriou, E. Giannini, B. W. Hoogenboom, C. Hess, T. Cren, and Ø. Fischer, Imaging the essential role of spin fluctuations in high-T_c superconductivity, Phys. Rev. Lett. **103**, 227001 (2009).
- [32] M. H. Hamidian, I. A. Firmo, K. Fujita, S. Mukhopadhyay, J. W. Orenstein, H. Eisaki, S. Uchida, M. J. Lawler, E.-A. Kim, and J. C. Davis, Picometer registration of zinc impurity states in $Bi_2Sr_2CaCu_2O_{8+\delta}$ for phase determination in intra-unit-cell Fourier transform STM, New J. Phys. 14, 053017 (2012).
- [33] See Supplemental Material at http://link.aps.org/supplemental/ 10.1103/PhysRevB.110.224501 for analysis of Bi-2212 sample, optimally doped and overdoped Bi-2201 samples, and redistribution of the gaps by STUFF algorithm compared to the traditional algorithm.
- [34] P. A. Lee, Amperean pairing and the pseudogap phase of cuprate superconductors, Phys. Rev. X 4, 031017 (2014).
- [35] Z. Dai, Y.-H. Zhang, T. Senthil, and P. A. Lee, Pair-density waves, charge-density waves, and vortices in high- *T_c* cuprates, Phys. Rev. B **97**, 174511 (2018).
- [36] Z. Dai, T. Senthil, and P. A. Lee, Modeling the pseudogap metallic state in cuprates: Quantum disordered pair density wave, Phys. Rev. B 101, 064502 (2020).
- [37] K. Seo, H.-D. Chen, and J. Hu, Complementary pair-density-wave and *d*-wave-checkerboard orderings in high-temperature superconductors, Phys. Rev. B **78**, 094510 (2008).
- [38] Z. Tešanović, Charge modulation, spin response, and dual hofstadter butterfly in high- T_c cuprates, Phys. Rev. Lett. **93**, 217004 (2004).
- [39] M. R. Norman and J. C. S. Davis, Quantum oscillations in a biaxial pair density wave state, Proc. Natl. Acad. Sci. USA 115, 5389 (2018).
- [40] S. E. Sebastian and C. Proust, Quantum oscillations in hole-doped cuprates, Annu. Rev. Condens. Matter Phys. **6**, 411 (2015).
- [41] M. Zelli, C. Kallin, and A. J. Berlinsky, Quantum oscillations in a π-striped superconductor, Phys. Rev. B 86, 104507 (2012).
- [42] Y. Caplan and D. Orgad, Quantum oscillations from a pairdensity wave, Phys. Rev. Res. 3, 023199 (2021).
- [43] D. Chakraborty, M. Grandadam, M. H. Hamidian, J. C. S. Davis, Y. Sidis, and C. Pépin, Fractionalized pair density wave in the pseudogap phase of cuprate superconductors, Phys. Rev. B 100, 224511 (2019).
- [44] M. Grandadam, D. Chakraborty, and C. Pépin, Fractionalizing a local pair density wave: A good "recipe" for opening a pseudogap, J. Supercond. Nov. Magn. 33, 2361 (2020).

- [45] S. Wang, P. Choubey, Y. X. Chong, W. Chen, W. Ren, H. Eisaki, S. Uchida, P. J. Hirschfeld, and J. C. S. Davis, Scattering interference signature of a pair density wave state in the cuprate pseudogap phase, Nat. Commun. 12, 6087 (2021).
- [46] P. Corboz, S. R. White, G. Vidal, and M. Troyer, Stripes in the two-dimensional t-J model with infinite projected entangled-pair states, Phys. Rev. B **84**, 041108(R) (2011).
- [47] B.-X. Zheng, C.-M. Chung, P. Corboz, G. Ehlers, M.-P. Qin, R. M. Noack, H. Shi, S. R. White, S. Zhang, and G. K.-L. Chan, Stripe order in the underdoped region of the two-dimensional Hubbard model, Science 358, 1155 (2017).
- [48] J. L. Tallon, J. W. Loram, G. V. M. Williams, J. R. Cooper, I. R. Fisher, J. D. Johnson, M. P. Staines, and C. Bernhard, Critical doping in overdoped high-T_c superconductors: A quantum critical point? Phys. Status Solidi B 215, 531 (1999).
- [49] S. H. Naqib, J. R. Cooper, J. L. Tallon, and C. Panagopoulos, Temperature dependence of electrical resistivity of high- T_c cuprates—-from pseudogap to overdoped regions, Phys. C (Amsterdam, Neth.) **387**, 365 (2003).
- [50] E. Sterpetti, J. Biscaras, A. Erb, and A. Shukla, Comprehensive phase diagram of two-dimensional space charge doped Bi₂Sr₂CaCu₂O_{8+x}, Nat. Commun. **8**, 2060 (2017).

- [51] N. Mohanta, Chiral pair density wave as the precursor of pseudogap in kagome superconductors, Phys. Rev. B 108, L220507 (2023).
- [52] S. Tajima, T. Noda, H. Eisaki, and S. Uchida, *c*-axis optical response in the static stripe ordered phase of the cuprates., Phys. Rev. Lett. **86**, 500 (2001).
- [53] M. H. Hamidian, S. D. Edkins, S. H. Joo, A. Kostin, H. Eisaki, S. Uchida, M. J. Lawler, E.-A. Kim, A. P. Mackenzie, K. Fujita *et al.*, Detection of a cooper-pair density wave in Bi₂Sr₂CaCu₂O_{8+x}, Nature (London) **532**, 343 (2016).
- [54] S. D. Edkins, A. Kostin, K. Fujita, A. P. Mackenzie, H. Eisaki, S. Uchida, S. Sachdev, M. J. Lawler, E.-A. Kim, J. C. Séamus Davis *et al.*, Magnetic field–induced pair density wave state in the cuprate vortex halo, Science 364, 976 (2019).
- [55] H. Zhao, R. Blackwell, M. Thinel, T. Handa, S. Ishida, X. Zhu, A. Iyo, H. Eisaki, A. N. Pasupathy, and K. Fujita, Smectic pairdensity-wave order in EuRbFe₄As₄, Nature (London) 618, 940 (2023).
- [56] Z. Du, H. Li, S. H. Joo, E. P. Donoway, J. Lee, J. C. S. Davis, G. Gu, P. D. Johnson, and K. Fujita, Imaging the energy gap modulations of the cuprate pair-density-wave state, Nature (London) 580, 65 (2020).